12th ANKARA INTERNATIONAL AEROSPACE CONFERENCE **AIAC-2023-013**
13-15 September 2023 - Online, Ankara, TURKIYE

FIXED WING AIRCRAFT AUTOMATIC LANDING WITH INTEGRAL ACTION MODEL PREDICTIVE CONTROL

Talha Ulukir* and Yusuf Sincak†
Turkish Aerospace
Ankara, Turkiye

Ilker Ustoglu‡
Istanbul Technical Univesity
Istanbul, Turkiye

ABSTRACT

The part of fixed-wing aircraft with the highest accident rate during a flight is the landing phase. During landing, the aircraft is exposed to a high amount of disturbance, however, an attempt is made to follow a trajectory. Fully autonomous landing systems can make it easier to pass parts that are difficult for the pilot. In this study, the Model Predictive Control method was used as the controller and the main reason for choosing this method is to find the optimal solution in case of exposure of the system to disturbances without reaching the physical limits. Although the MPC method is basically a regulator function, it can be modified and used in reference tracking, as in this study. In this case, a multi-input multi-output controller that both follows the reference and determines the optimum control signal by knowing the system constraints is obtained, and many problems of the descent phase are handled at once.

INTRODUCTION

Disturbances acting on the aircraft during the automatic landing phase may cause system variables or system inputs to reach limits. This situation causes the aircraft to be unresponsive to disruptors after that point. For the solution of this problem, it will be advantageous to use the MPC method, which takes into account the constraints, and will provide the optimum solution within the constraints.

Generally, MPC calculates the next output value of the system using the current and previous input signal of the system. In order to minimize the error between the output of the system and the reference value, the most appropriate control (input) signal sequence is calculated and applied to the system. That is, MPC is a controller that calculates the necessary control sequence to optimize the future behavior of a system. The receding horizon control method used is used to predict the future output and calculates the optimum control command at the horizon width under this condition.

AIRCRAFT MODEL

The aircraft model to be used in the thesis is GTM (GenericTransport Model), which can also be

*Flight Control Law and Algorithm Design Engineer, UAV Division, Email: talha.ulukir@tai.com.tr
†Flight Control Law and Algorithm Design Engineer, UAV Division, Email: yusuf.sincak@tai.com.tr
‡Assoc. Prof. Dr.,Control and Automation Engineering, Email: ustoglui@itu.edu.tr

found in the NASA Technology Transfer Program. NASA Aviation Safety Program conducted studies with the T-2 tail numbered aircraft, which was developed within the scope of the General Transport Model, in order to examine the situations caused by loss of control in aircraft. It is aimed to develop flight control technologies that can provide control in case of loss of control due to damage and malfunction in this aircraft. In addition to the aircraft non-linear model, varying behaviors in error scenarios are also included in the model. After the classical aircraft modeling studies, the flights were carried out and the final version of the model was obtained. [Wolowicz, C. H., Bowman, J. S., Gilbert, W. P. (1979)]

System Characteristics

When the aircraft linear model is obtained, longitudinal and lateral dynamics are easily separable for fixed-wing aircraft. We can interpret the characteristics of the aircraft according to the location of the poles of the linear model of the aircraft, which is separated longitudinally and laterally in conventional aircraft traveling at subsonic speeds.

The decoupled longitudinal state space matrices of the system are as follows.

$$\begin{bmatrix} \dot{V} \\ \dot{\alpha} \\ \dot{q} \\ \dot{\theta} \end{bmatrix} = \begin{pmatrix} -0.727 & 11.2101 & 0.2012 & -19.0598 \\ -0.0076 & -2.0847 & 0.9372 & 0.0047 \\ -0.0145 & -24.7317 & -3.0278 & 0 \\ 0 & 0 & 1 & 0 \end{pmatrix} \begin{bmatrix} V \\ \alpha \\ q \\ \theta \end{bmatrix} + \begin{pmatrix} -0.0181 & 0.04 \\ -0.0038 & 0 \\ -0.6374 & 0.0091 \\ 0 & 0 \end{pmatrix} \begin{bmatrix} \delta_e \\ \delta_t \end{bmatrix}$$

and lateral state space matrices of the system are as follows.

$$\begin{bmatrix} \dot{\beta} \\ \dot{p} \\ \dot{r} \\ \dot{\phi} \end{bmatrix} = \begin{pmatrix} -0.4689 & 0.1156 & -0.9821 & 0.2698 \\ -72.6178 & -5.1149 & 2.3352 & 0 \\ 22.3184 & -0.472 & -1.2413 & 0 \\ 0 & 1 & 0.0978 & 0 \end{pmatrix} \begin{bmatrix} \beta \\ p \\ r \\ \phi \end{bmatrix} + \begin{pmatrix} 0 & 0.0027 \\ -0.6594 & 0.1724 \\ -0.0404 & -0.3466 \\ 0 & 0 \end{pmatrix} \begin{bmatrix} \delta_a \\ \delta_r \end{bmatrix}$$

Accordingly, the modes of longitudinal dynamics are as follows.

Mode	Pole	Damping	Frequency (rad/seconds)	Time Constant (seconds)
Phugoid Mode	$-0.0229 + 0.287$i	0.0796	0.288	43.6
Phugoid Mode	$-0.0229 - 0.287$i	0.0796	0.288	43.6
Short-Period Mode	$-3.03 + 6.5$i	0.422	7.17	0.330
Short-Period Mode	$-3.03 + 6.5$i	0.422	7.17	0.330

Table 1: Longitudinal Modes

and the modes of lateral dynamics are as follows.

Mode	Pole	Damping	Frequency (rad/seconds)	Time Constant (seconds)
Spiral Mode	-0.0448	1.00	0.0448	22.3
Dutch-Roll Mode	$-0.857 + 6.26$	0.136	6.31	1.17
Dutch-Roll Mode	$-0.857 - 6.26$	0.136	6.31	1.17
Roll Mode	-6.62	1.00	6.62	0.151

Table 2: Lateral Modes

When the system modes are examined, it is seen that the aircraft is stable and the modes are distributed in accordance with the classical polar arrangement.

METHOD

Integral Action Model Predictive Control

Let the expression of a linear time-invariant system in discrete time space be as follows:

$$x_{k+1} = A \cdot x_k + B \cdot u_k, y_k = C \cdot x_k$$

Here x_k denotes the states of the system and u_k denotes the inputs of the system. In the model predictive control method, obtaining the optimal control sign of the system at a certain horizon can be expressed with a quadratic function.

$$J_0\left(x_0, U\right) = \sum_{k=0}^{Np-1} x_k^T * Q * x_k + \sum_{k=0}^{Nc-1} u_k^T * R * u_k$$

In quadratic function; Np denotes the predict horizon of the system, Nc denotes the control horizon of the system, while x_0 denotes the state vector. The main purpose in model predictive control is to calculate the U vector that will minimize this quadratic function. Q, P and R weighting matrices are also important in the calculation of this vector. While the Q matrix expresses the weighting between the states of the system, the R matrix expresses the weighting between the inputs of the system.

The classical state space MPC solution is in the form of a regulator and is not fully suitable for reference tracking. Therefore, the integral-action MPC approach is used in this study. With this sub-solution, the MPC structure will be suitable to follow the given references without any steady-state error. For this, we need to manipulate the matrices of the system and make them augmented. [Rossiter,2017;Wang,2009]

$$\begin{bmatrix} \Delta x(k+1) \\ y(k+1) \end{bmatrix} = \overbrace{\begin{bmatrix} A & o^T \\ CA & 1 \end{bmatrix}}^{A_{aug}} \overbrace{\begin{bmatrix} \Delta x(k) \\ y(k) \end{bmatrix}}^{x(k)} + \overbrace{\begin{bmatrix} B \\ CB \end{bmatrix}}^{B_{aug}} \Delta u(k)$$

$$y(k) = \overbrace{\begin{bmatrix} o & 1 \end{bmatrix}}^{C_{aug}} \begin{bmatrix} \Delta x(k) \\ y(k) \end{bmatrix}$$

Based on the state-space form, the future state variables of the system can be expressed as follows:

$$x(k+1) = Ax(k) + B(\Delta u(k) + u(k-1))$$

and the quadratic function for augmented state space matrices can be written as follows.

$$J_0\left(x_0, U\right) = \sum_{k=0}^{Np-1} \left(ref - y_k^T\right) * Q * (ref - y_k) + \sum_{k=0}^{Nc-1} u_k^T * R * u_k$$

If the equation given for state is to be generalized:

$$\begin{aligned} x(k+\mathrm{Np}) = A^{\mathrm{Np}}x(k) &+ \left(A^{\mathrm{Np}-1}B + A^{\mathrm{Np}-2}B + \cdots + A^2B + AB + B\right)\Delta u(k) \\ &+ \left(A^{\mathrm{Np}-2}B + A^{\mathrm{Np}-3}B + \cdots + AB + B\right)\Delta u(k+1) \\ &+ \left(A^{\mathrm{Np}-3}B + A^{\mathrm{Np}-4}B + A^{\mathrm{Np}-5}B + \cdots + B\right)\Delta u(k+2) \\ &+ \left(A^{\mathrm{Np}-1}B + A^{\mathrm{Np}-2}B + \cdots + A^{\mathrm{Np}-\mathrm{Nc}}B + AB + B\right)u(k-1) \end{aligned}$$

Based on the state-space form, the future outputs of the system can be expressed as follows:

$$y(k+1) = CAx(k) + CB(\Delta u(k) + u(k-1))$$

If the equation given for state is to be generalized:

$$y(k+\mathrm{Np}) = CA^{\mathrm{Np}}x(k) + \left(CA^{\mathrm{Np}-1}B + CA^{\mathrm{Np}-2}B + \cdots + CA^2B + CAB + CB\right)\Delta u(k)$$
$$+ \left(CA^{\mathrm{Np}-2}B + CA^{\mathrm{Np}-3}B + \cdots + CAB + CB\right)\Delta u(k+1)$$
$$+ \left(CA^{\mathrm{Np}-3}B + CA^{\mathrm{Np}-4}B + CA^{\mathrm{Np}-5}B + \cdots + CB\right)\Delta u(k+2)$$
$$+ \left(CA^{\mathrm{Np}-1}B + CA^{\mathrm{Np}-2}B + \cdots + CA^{\mathrm{Np}-\mathrm{Nc}}B\right)u(k-1)$$

Note that all variables can be expressed in terms of previous outputs of the system and future control signals. If the output variables are expressed as a vector:

$$Y = \left[y\left(k_i+1 \mid k_i\right) y\left(k_i+2 \mid k_i\right) y\left(k_i+3 \mid k_i\right) \ldots y\left(k_i+N_p \mid k_i\right)\right]^T$$

$$\Delta U = \left[\Delta u\left(k_i\right) \Delta u\left(k_i+1\right) \Delta u\left(k_i+2\right) \ldots \Delta u\left(k_i+N_c-1\right)\right]^T$$

With these vectors, we can express the prediction horizon of the system in a simpler way.

$$Y = Fx\left(k_i\right) + \mathrm{H}\Delta U$$

where

$$F = \begin{bmatrix} CA \\ CA^2 \\ CA^3 \\ \vdots \\ CA^{N_p} \end{bmatrix}; \mathrm{H} = \begin{bmatrix} CB & 0 & 0 & \ldots & 0 \\ CAB & CB & 0 & \ldots & 0 \\ CA^2B & CAB & CB & \cdots & 0 \\ \vdots & & & & \\ CA^{N_p-1}B & CA^{N_p-2}B & CA^{N_p-3}B & \ldots CA^{N_p-N_c}B & \end{bmatrix}$$

Let ref_s the reference value given to the system be extended along the forecast horizon. Accordingly, we can also revise the quadratic function equation.

$$J = \left(ref_s - Y\right)^T \left(ref_s - Y\right) + \Delta U^T \mathrm{R}\Delta U$$

When we combine previous equation and Y, we obtain

$$J = \left(ref_s - Fx\left(k_i\right) + \mathrm{H}\Delta U\right)^T \left(ref_s - Fx\left(k_i\right) + \mathrm{H}\Delta U\right) + \Delta U^T \mathrm{R}\Delta U$$

The place where a quadratic function is the minimum for the unconstrained solution is located where its first derivative is 0, accordingly:

$$\frac{\partial J}{\partial \Delta U} = -2\Phi^T \left(ref_s - Fx\left(k_i\right)\right) + 2\left(\Phi^T\Phi + \bar{R}\right)\Delta U = 0$$

and the control sign for the unconstrained solution can be expressed with the prediction matrices F and H:

$$\Delta U = \left(\mathrm{H}^T\mathrm{H} + \bar{R}\right)^{-1} \Phi^T \left(ref_s - Fx\left(k_i\right)\right)$$

For the constrained solution of the quadratic function, the first derivative of the objective function will not be sufficient, here the control command that minimizes the objective function can be calculated with different optimization solution methods. Another thing as important as performance in control system design is the stability of the system. Since the control coefficients of control loops are certain in Explicit solutions, open loop and closed loop stability analyzes can be made by

breaking the loops from various places. In the Model Predictive Control method, where the online control signal is obtained, it is not possible to do this analysis with classical methods. [Mayne, Rawlings, Rao, Scokaert (2000)] made some recommendations for stability analysis for MPC. For this, all eigenvalues of the A matrix of the state-space model are in the unit-circle, the weighting matrix $Q \geq 0$ and the Lyapunov matrix $\bar{Q} \geq 0$ ensure the stability of the system.

In the controller design, constraints were added on the control signals, while the constraints were added, the boundaries of the system inputs (control surfaces) were taken as limits and the MATLAB quadprog function was used for the constrained solution.

LANDING ALGORITHM

Eligibility for Landing

Before the flare altitude of the aircraft, the target speed $V_{STALL} * 1.3$ was trimmed with different flight path angles, and instant throttle usages were examined in these trim results. Depending on the designer's choice, any condition can be selected here, but at least 10 percent throttle usage is expected within the scope of this study. In this case, the maximum flight path angle of the aircraft with respect to the flare point was taken as -4 degrees, and the aircraft transferred to the landing autopilot were aimed to land at angles up to this angle. (Figure 1)

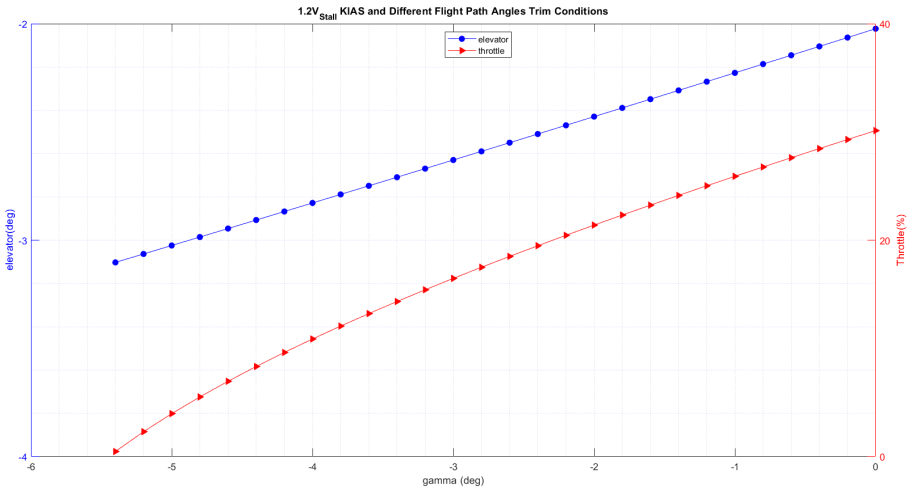

Figure 1: Different Flight Path Angle and Constant Speed Trim Results for Actuators

Within the scope of the thesis, a ramp-like approach is carried out for the glide phase and transferred to the flare phase. Accordingly, aircraft in conditions with an angle value (FPA_{glide}) between -4 degrees and 0 degrees as a result of the simple calculation below are suitable for automatic landing.

$$-\frac{(h - h_{flare})}{R} = FPA_{glide}$$

where R is the resultant distance on the horizontal axes to the flare point of the aircraft.
The speed condition for suitability for landing can be formulated as follows.

$$ArriveTime_{Estimated} = \frac{R}{\frac{V+V_{flare}}{2}}$$

$$\frac{V - V_{flare}}{ArriveTime_{Estimated}} < deceleration_{target}$$

With this equation, it is aimed that the aircraft will slow down with a speed of approximately $deceleration_{target}$ m/s until the transition time to the flare phase. The $deceleration_{target}$ value can be selected by the designer, and 10 for 0 degrees flight path angle and 15 for 4 degrees flight path angle were selected within the scope of the study. Linear interpolation is used for the angles in between. Accordingly, a landing distance is expected at different speeds and angles as in the (Figure 2).

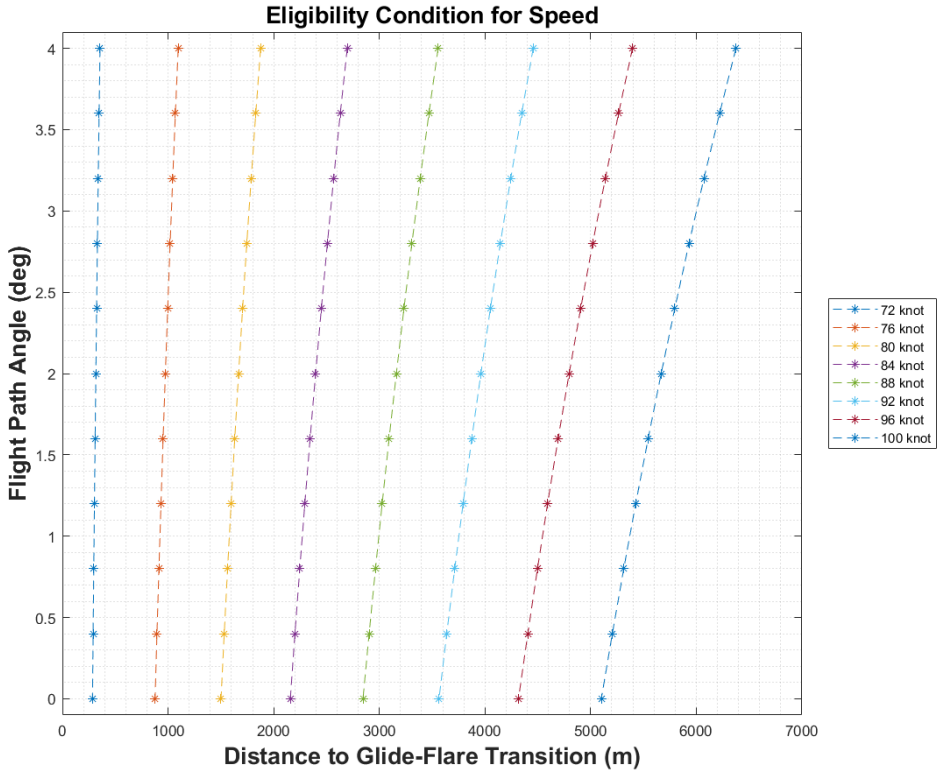

Figure 2: Different Flight Path Angle and Constant Speed Trim Results for Actuators

Reference Calculations

Pitch Angle Reference Generation: For glide phase, a function that generates a command from the starting altitude to the runway altitude is used according to the current vertical speed of the aircraft after the landing.

$$h_{cmd}(i) = \frac{h_{glide} - h_{touchdown}}{\dot{h}} \Delta \mathrm{t} + h_{cmd}(i-1)$$

and

$$H_{cmd}(0) = H_{GlideStart}$$

For flare phase, a control architecture in which the pitch reference due to altitude error is generated in the longitudinal motion [Stevens, B. L., Lewis, F. L., Johnson, E. N. (2015)] will be preferred for automatic landing. The first order command generator structure, in which the altitude reference is reduced exponentially, will be used for the speed reference in the same way. A value of 0 will be fed as the altitude reference, while $1.3 * V_{stall}$ will be fed for the speed reference as in the [FAA,2016]. V_{stall} for the respective aircraft has been calculated as follows:

$$V_{STALL} = \sqrt{\frac{2W * g}{\rho A C_{L_{MAX}}}}$$

where

$$W = Weight$$

$$\rho = AirDensity$$

$$\mathrm{A} = WingArea$$

$$C_{L_{MAX}} = MaximumLiftCoefficient$$

For GTM-T2 Aircraft

$$\mathrm{W} = 78\mathrm{lb}$$

$$\rho = 0.0765\frac{\mathrm{lb}}{\mathrm{ft}^3}$$

$$\mathrm{A} = 5.9018\mathrm{ft}^2$$

$$C_{L_{MAX}} = 1.3541,\ \mathrm{g} = 32.17404855643\frac{\mathrm{ft}}{\mathrm{s}^2}$$

$$V_{STALL} = \sqrt{\frac{2 * 57.75\mathrm{lb} * 32.17404855643\frac{\mathrm{ft}}{\mathrm{s}^2}}{0.0765\frac{\mathrm{lb}}{\mathrm{ft}^3} * 5.9018\mathrm{ft}^2 * 1.3541}}$$

$$V_{STALL} = 95.2349\frac{\mathrm{ft}}{\mathrm{s}} = 53.7385\mathrm{kts}$$

$$LandingSpeed = V_{STALL} * 1.3 = 69.86\mathrm{kts} \cong 70\mathrm{kts}$$

With the onset of the flare phase (approximately the last 50 feet), the aircraft begins to descend for a soft kickback towards the landing point, the descent acceleration at the touchdown point should be less than $-2\frac{feet}{\mathrm{sec}}$. In order to meet the required requirements, the required τ should be selected in the equation below.

$$\dot{h} = \frac{1}{\tau}h + r$$

$$h(0) = h_0$$

$$h_{cmd}(t) = h_0 e^{(-t/\tau_{alt})}$$

The following equation is used to convert the altitude error to pitch angle reference:

$$(h_{cmd} - h) * K_{hdot} = \dot{h}_{ref}$$

$$atan\left(\frac{\dot{h}_{ref}}{Speed}\right) = \gamma_{ref}$$

$$\gamma_{ref} + \alpha_{actual} = \theta_{ref}$$

Speed Reference Generation:

The reference of velocity, which is another variable in the longitudinal plane, is created in a similar way to the altitude reference. While the speed reference is commanded to ramp down to $V_{STALL} * 1.3$ during the glide-flare transition, there is an exponential speed reference to descend to $V_{STALL} * 1.1$ with the flare. The reason for the $V_{STALL} * 1.1$ command of the flare moment is for the aircraft to descend to the maximum speed that will provide lift during wheel landing and not to take off again after wheel landing.

A similar speed reference generation approach is used in both phases of landing. The estimated remaining time is calculated by dividing the difference between the altitude at which the phase starts and the altitude at which it will end by the vertical velocity. The rate of the deceleration curve is obtained by dividing this remaining time by the difference between the ending and starting

speeds. By decreasing the speed obtained from the speed at the beginning of the relevant phase, the aircraft is at the desired speed at the end of the phase.

$$V_{cmd_{glide}}(i) = \frac{V_{glide} - V_{flare}}{\frac{h_{glide} - h_{flare}}{h}} \Delta \mathrm{t} + V_{cmd}(i-1)$$

and

$$V_{cmd_{flare}}(i) = \frac{V_{flare} - V_{touchdown}}{\frac{h_{flare} - h_{touchdown}}{h}} \Delta \mathrm{t} + V_{cmd}(i-1)$$

Roll and Sideslip Angle Reference Generation: In the lateral-directional motion, an outer loop controller that generates a roll reference due to heading angle error like [Blakelock. (1991)] will be preferred. The heading reference of the aircraft will be obtained from the angle at which the aircraft will land and the distance it takes on the lateral axis. Before the flare phase, the heading control is done with the Roll control, and with the flare phase, zero is commanded as a roll reference so that the wings of the aircraft are straight and the wheel is not placed with the bank angle. Along with Flare, beta is used to follow the heading reference. Reference models to be used for lateral control before flare phase are as follows:

$$\varphi_{cmd} = \left(- \left(\frac{\frac{V_t * \sin\left(\Psi - \Psi_{ref}\right)}{S}}{R} \right) * K_\lambda - \Psi \right) * \frac{Speed}{\tau_{heading} * g}$$

R is distance to glide-flare transition point. In the last part of the landing (flare), the aircraft's being in the lying position may cause asymmetries at the time of landing, therefore the method used to hold the line after the flare is changed. Reference models to be used for lateral control after flare phase are as follows:

$$\varphi_{cmd} = 0$$

$$\beta_{cmd} = (\Psi_{ref} - \Psi) * K_{heading2beta}$$

$$\beta_{ref}(t) = (\beta_{trim} - \beta_{cmd}) * e^{\left(-\frac{t}{\tau_{sideslip}}\right)} + \beta_{cmd}$$

Controller Design

Weighting Matrices

Bryson's rule was used in the weighting matrices used in the solution of the Quadratic problem.According to this method, a simple and reasonable choice for the matrices $\bar{Q}$ and $\tilde{R}$ in (20.2) is given by Bryson's rule [6, p. 537]. Select $\bar{Q}$ and $\tilde{R}$ diagonal, with

$$\mathbf{Q} = diag\left\{ \frac{\alpha_1^2}{x_{1^2_{\max}}^2}, \frac{\alpha_2^2}{x_{2^2_{\max}}^2}, \quad \cdots, \frac{\alpha_n^2}{x_{n_{\max}}^2} \right\}$$

$$\mathbf{R} = \rho diag\left\{ \frac{\beta_1^2}{u_{1^2_{\max}}^2}, \frac{\beta_2^2}{\beta_{2^2_{\max}}^2}, \quad \cdots, \frac{\beta_m^2}{u_{m_{\max}}^2} \right\}$$

which corresponds to the following criterion

$$J_{\mathrm{LQR}} := \int_0^\infty \left(\sum_{i=1}^{\ell} \bar{Q}_{ii} z_i(t)^2 + \rho \sum_{j=1}^{m} \bar{R}_{jj} u(t)^2 \right) dt.$$

In essence, Bryson's rule scales the variables that appear in J_{LQR} so that the maximum acceptable value for each term is 1 . This is especially important when the units used for the different

components of u and z make the values for these variables numerically very different from each other.

Longitudinal Controller Design

In the longitudinal autopilot design, altitude and speed hold autopilot are designed. (Figure 3) Pitch angle reference was obtained by passing the altitude error PI control, the Model Predictive Control structure was used for Theta and Speed holding as the inner loop controller.

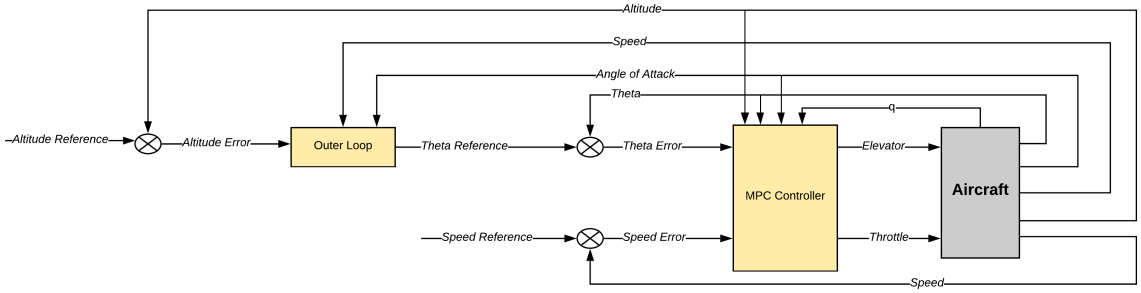

Figure 3: Longitudinal Landing Architecture

Weighting matrices obtained respect to table in below. Longitudinal autopilot Q and R weighting

Parameter	Value	Usage
α_1	0.4	Speed Weight
α_2	0.6	Pitch Weight
x_{1max}	9.5618	Speed Maximum
x_{2max}	0.0296	Pitch Maximum
β_1	0.996	Elevator Weight
β_2	0.004	Throttle Weight
u_{1max}	30	Elevator Maximum
u_{2max}	100	Throttle Maximum

Table 3: Parameters which selected for Longitudinal MPC

matrices for the Model Predictive Control are defined as follows.

$$Q = \begin{bmatrix} 0.00443 & 0 \\ 0 & 684.7243 \end{bmatrix} R = \begin{bmatrix} 68.889 & 0 \\ 0 & 0.04 \end{bmatrix}$$

When the weighting matrices used for longitudinal autopilot are examined with Lyapunov Theorem:

$$\bar{Q} = \begin{bmatrix} 314.2895 & -3382.3 & 222.6021 & 3346 \\ -3382.3 & 839540 & -72299 & -992840 \\ 222.6021 & -72299 & 6689.7 & 879710 \\ 3346 & -99284 & 87971 & 120110 \end{bmatrix}$$

$$\lambda(\bar{Q}) = \begin{bmatrix} 234.1146 & 285.607 & 11256 & 2035900 \end{bmatrix}$$

However, in the controller designed discrete linear model of the system, the eigenvalues of the system are in the unit circle, their locations:

$$\begin{bmatrix} 0.986 + 0.023i & 0.986 - 0.023i & 0.9995 + 0.0016i & 0.9995 - 0.0016i \end{bmatrix}$$

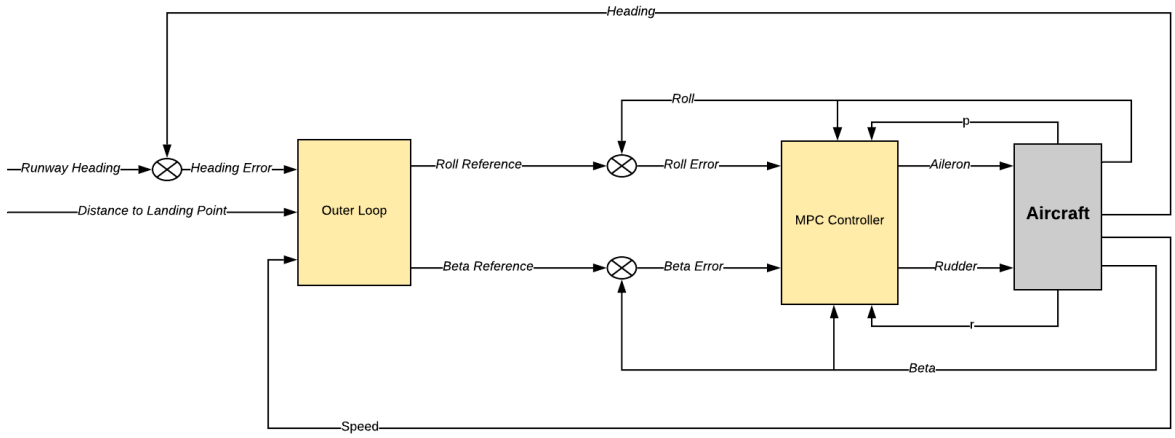

Figure 4: Lateral Landing Architecture

Lateral Controller Design

In the lateral autopilot design, heading angle and sideslip(beta) hold autopilot are designed. (Figure 4) Roll reference was obtained by passing the heading error, the Model Predictive Control structure was used for Roll and Beta holding as the inner loop controller. Weighting matrices obtained respect to table in below. Lateral autopilot Q and R weighting matrices for the Model Predictive

Parameter	Value	Usage
α_1	0.2	Roll Weight
α_2	0.8	Sideslip Weight
$\mathrm{x_{1max}}$	30	Roll Maximum
$\mathrm{x_{2max}}$	30	Sideslip Maximum
β_1	0.8	Aileron Weight
β_2	0.2	Rudder Weight
$\mathrm{u_{1max}}$	0.5236	Aileron Maximum
$\mathrm{u_{2max}}$	0.5236	Rudder Maximum

Table 4: Parameters which selected for Lateral MPC

Control are defined as follows.

$$Q = \begin{bmatrix} 4 & 0 \\ 0 & 1 \end{bmatrix} R = \begin{bmatrix} 500 & 0 \\ 0 & 500 \end{bmatrix}$$

When the weighting matrices used for longitudinal autopilot are examined with Lyapunov Theorem:

$$\bar{Q} = \begin{bmatrix} 165520 & -364010 & -20155 & -25375 \\ -36401 & 32380 & 10433 & 21907 \\ -11502 & 10433 & 34284 & 70547 \\ -2575 & 21907 & 70547 & 14930 \end{bmatrix}$$

$$\lambda(\bar{Q}) = \begin{bmatrix} 161.219 & 7552.5 & 120390 & 190570 \end{bmatrix}$$

However, in the controller designed discrete linear model of the system, the eigenvalues of the system are in the unit circle, their locations:

$$\begin{bmatrix} 0.9739 & 0.9878 - 0.0301i & 0.9878 + 0.0301i & 0.9988 \end{bmatrix}$$

Parameter	Value
Np	40
Nc	1
K_{hdot}	1
$H_{cmd}(Flare)$	50
τ_{alt}	25
$\tau_{heading}$	30
$K_{heading2beta}$	-1
K_{λ}	1

Table 5: Parameters which selected by designer

RESULTS AND DISCUSSION

One of the most important performance criteria of the Online Model Predictive Control method is the speed of solution of the problem. Within the scope of automatic descent control problem, control signals created continuously by the state-space Model Predictive Control method were used. While the system is running for 0.0005s, the sampling time of the control structure is chosen as 0.02s. In the Model Predictive Control problem, the prediction horizon is 40 steps and the control horizon is 1 step. However, the average solution speed of the problem was 0.0013s. It is seen that the solution speed of the MPC problem is 14.9324 times the sampling time of the controller.

Longitudinal Motion

If we examine the performance of the longitudinal part of the automatic landing autopilot designed with MPC; (Figure 5) shows altitude hold, pitch hold, and speed hold throughout the entire descent. If we examine the speed holding before the flare phase; With the start of landing, the speed of the aircraft hovers around the speed reference and successfully follows the speed reference after about 20 seconds. Roaming around the reference here is one of the initial conditions of the simulation, and such a situation will not be seen in case of a rollover from another autopilot structure before the landing autopilot. After the flare transition (Figure 6), the speed hold is seen to be very successful. If we examine the control surface commands, there is no such thing as limiting in the commands and it is seen that the control is achieved with a successful one. If the altitude hold of the aircraft is examined; Altitude hold is seen as successful before the flare phase and there is no loss in theta grip. With the flare transition, the altitude reference comes exponentially rather than linearly, altitude hold is also very successful here, and the performance of the altitude tracking increases as the wheel approaches the put-down phase.

When the windy conditions are examined, in the longitudinal plane; It is seen that the aircraft has difficulty in keeping speed due to saturations in the throttle control command (Figure 7). In addition, the performance in altitude holding is seen to be satisfactory, especially after the transition to the flare phase, the altitude holding behavior continues despite the noise and distortion in the signals (Figure 8).

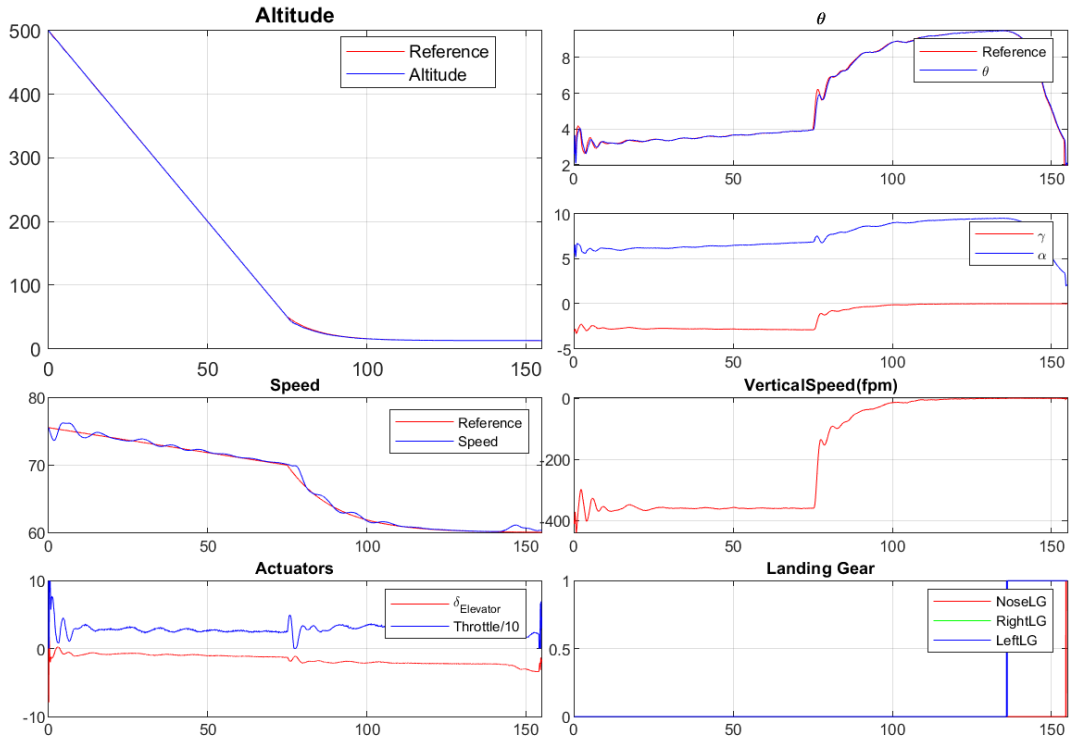

Figure 5: Longitunal Part Performance During Landing

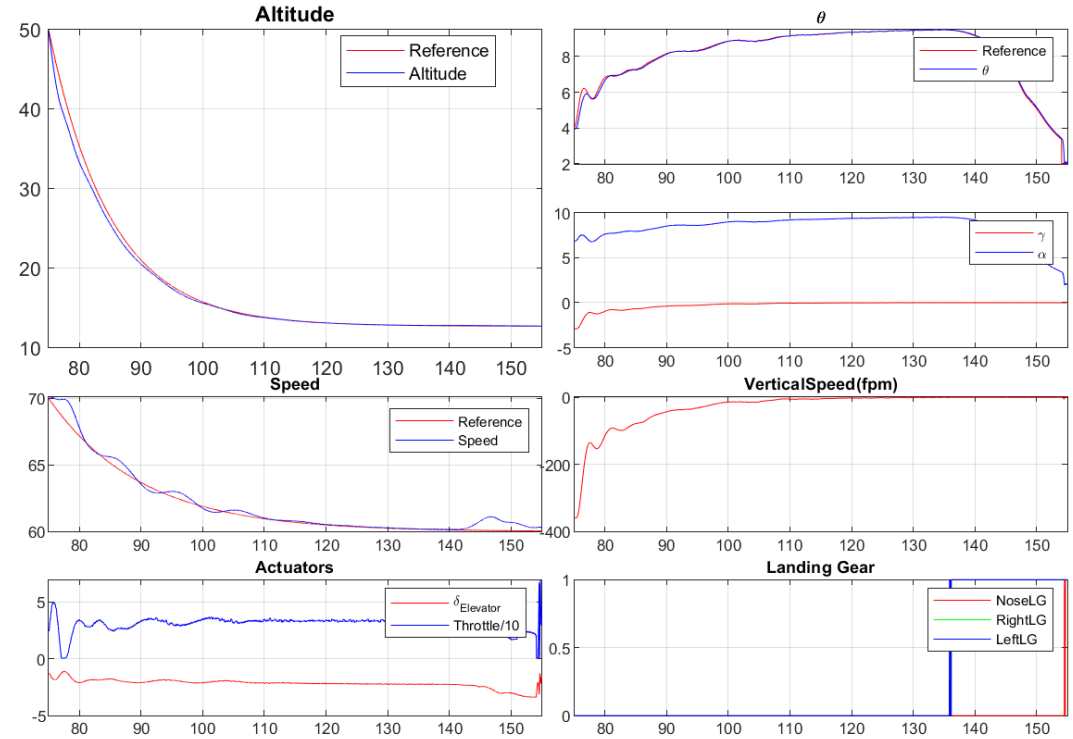

Figure 6: Longitunal Part Performance During Flare Phase

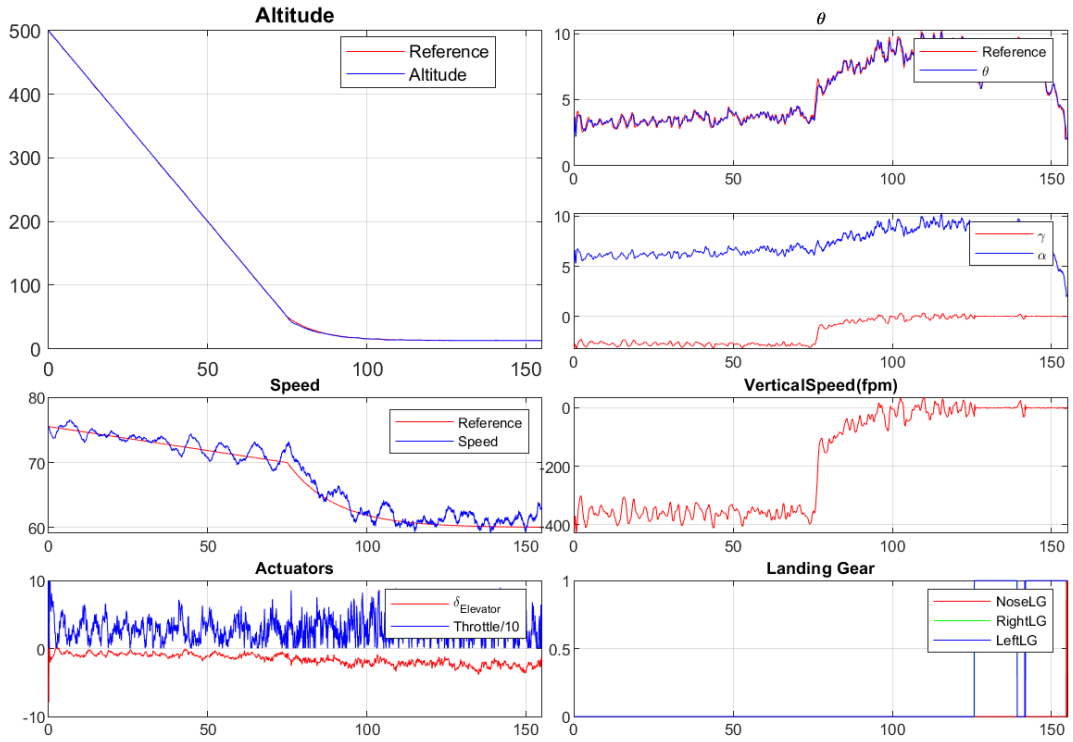

Figure 7: Longitunal Part Performance During Landing with Moderate Turbulance and 10knot Wind Condition

Lateral Motion

If we examine the performance of the lateral part of the landing autopilot (Figure 9) designed with the MPC controller; Before the flare phase, the tracking of the heading reference with the roll cycle is quite successful, and it is seen that it converges to the required heading reference before the flare transition. With the flare phase transition (Figure 10), it successfully follows the 0 degree reference of the roll angle. After the phase transition, a structure in which the heading reference tracking is made with beta is passed, it is seen that the beta reference tracking is followed successfully, at the end of the flare phase, there is a heading holding error of 0.1 degrees during wheel placement, this shows that the aircraft put the wheels in the same direction with the runway.

When the behavior in the lateral plane is examined under turbulence conditions, it is seen that there are serious deteriorations in the roll signal, especially after the flare phase, but it is seen that the aileron command in the aircraft control commands is working to correct this deterioration (Figure 11). In the glide phase, however, it is seen that it successfully follows the required roll command to follow the required heading reference, and the beta angle is observed to hover around 0 degrees in the same phase (Figure 12).

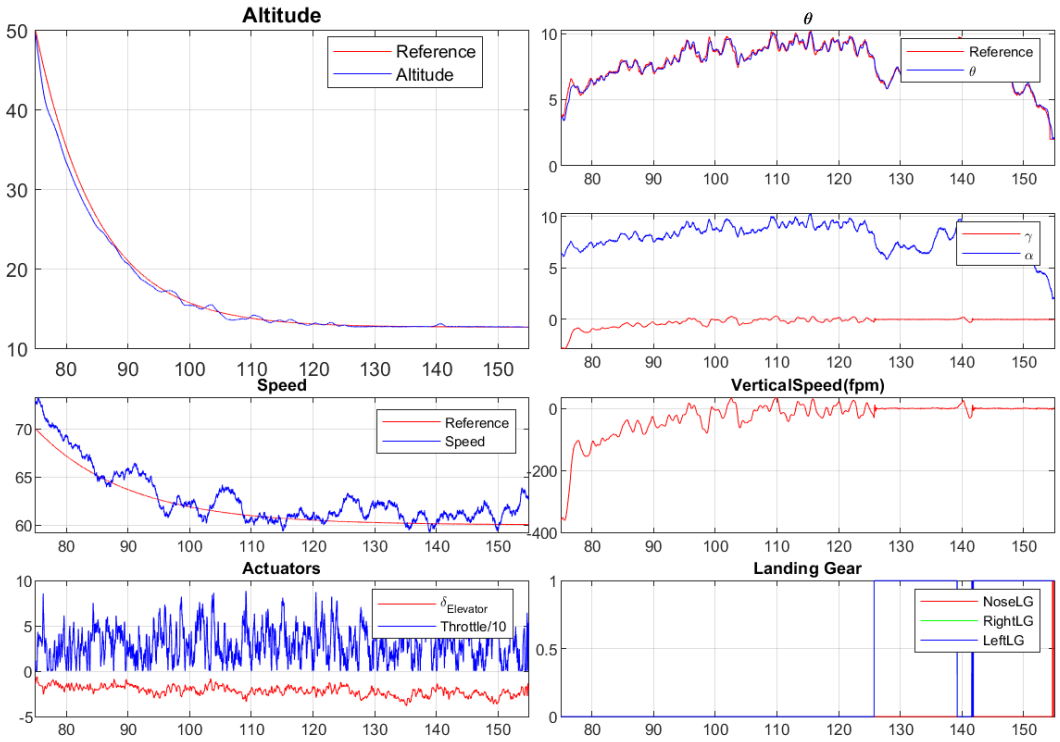

Figure 8: Longitunal Part Performance During Flare Phase with Moderate Turbulance and 10knot Wind Condition

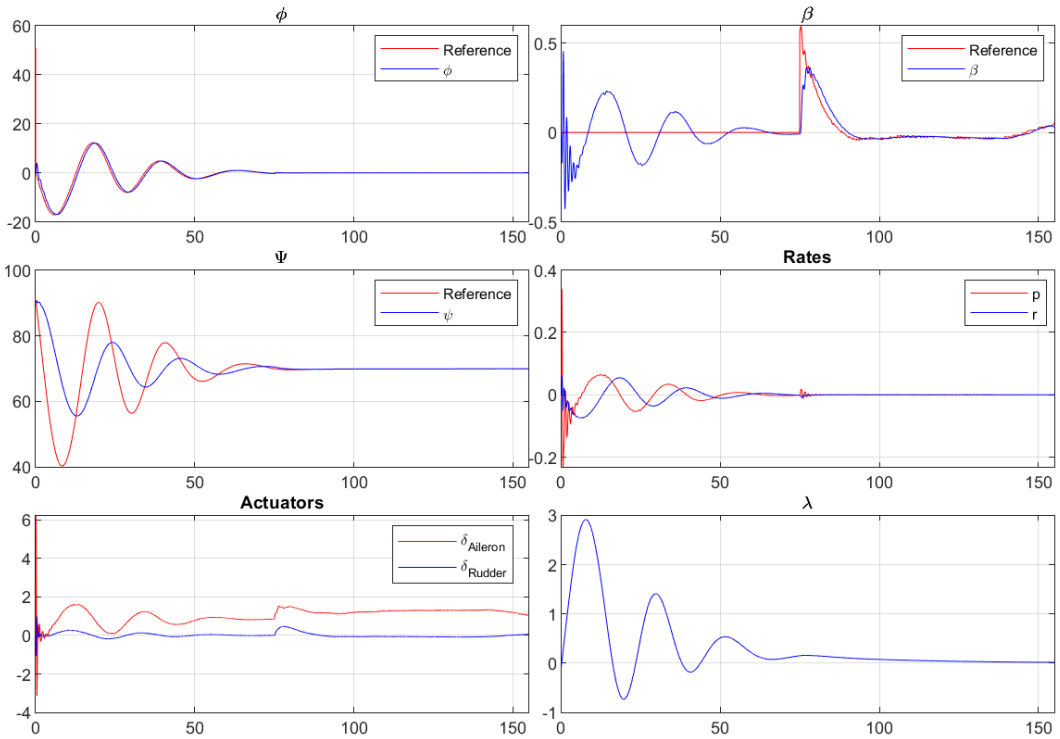

Figure 9: Lateral Part Performance During Landing

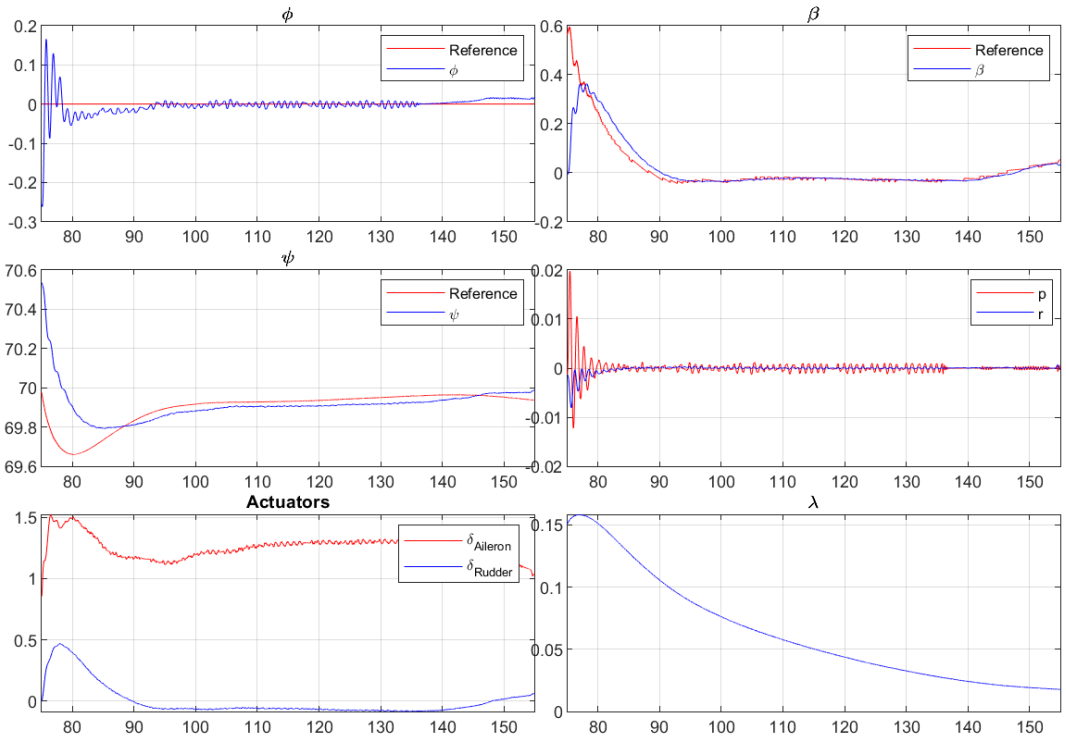

Figure 10: Lateral Part Performance During Flare Phase

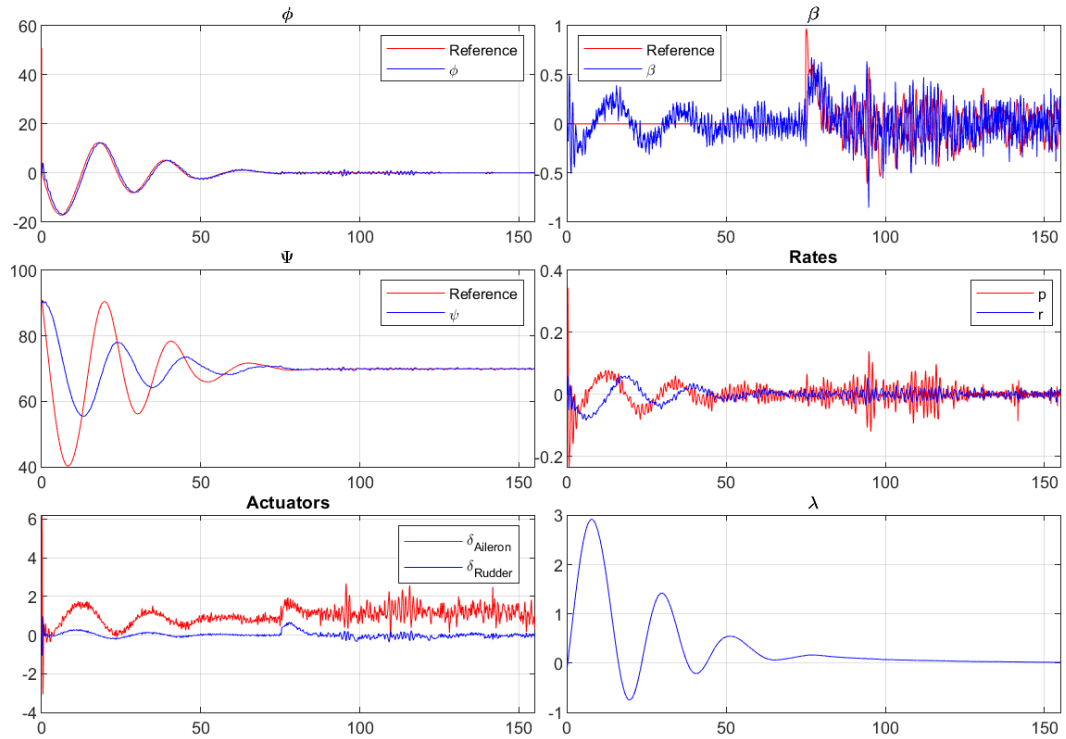

Figure 11: Lateral Part Performance During Landing with Moderate Turbulance and 10knot Wind Condition

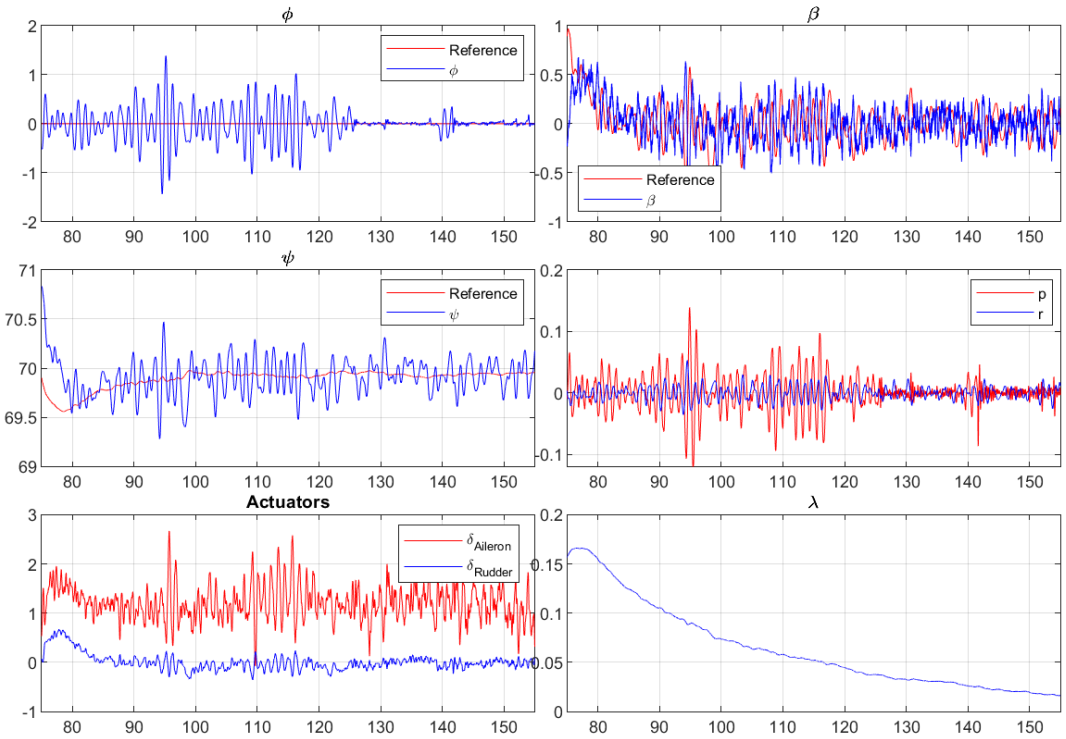

Figure 12: Lateral Part Performance During Flare Phase with Moderate Turbulance and 10knot Wind Condition

Compare

Landing architecture is compared with different control algorithms (PID, LQI and MPC) The system test conditions are as follows:
- Windshear: on, off.
- Turbulance: no turbulance, light turbulance, moderate turbulance.
- Damage state: no damage, rudder off, vertical tail off, left outboard flap off, left wingtip off, left elevator off, left stabilizer off.
- Damage time: glide start, flare start, touchdown start.
- Wind speed: 0, 5, 10, 15, 20, 25.
- Wind degree: 0, 60, 120, 180, 240, 300.

Tests were carried out for each controller under 4536 test conditions. Certain restrictions are placed on the evaluation of the test matrix:
- The altitude hold error is 5 meters below the all landing, the altitude hold error is 3 meters below the Flare phase.
- Speed hold error under 10 knots during the all landing, speed hold error under 5 knots in the Flare phase.
- Vario under 200 fpm when wheeled.
- The heading hold error is 20 degrees below the entire landing, the heading hold error is 10 degrees below the Flare phase.
- Lambda value less than 1 degree at the time of putting the wheel.

CONCLUSIONS

An automatic landing algorithm was designed with MPC, an online optimization and model-based

Controller	Total Succesful Landing	Total Test - Successful Landing Rate
PID	369	%8.13
LQI	498	%10.98
MPC	1050	%23.15

Table 6: Statistical compare of different control methods with same algoritm

control method, and it was seen that it gave successful results in the simulations. Although the integral-action MPC method used in the design requires the consistency of the real system with the mathematical model with its model-based structure, it offers a performance-enhancing solution with its multi-input, multi-output structure and model estimation that progresses at every step. In addition to the error minimization principle in the MPC structure, the integral effect added to the system facilitates success in reference tracking.

The fact that the PID controller is in a single-input, single-output structure and the LQI controller calculates the optimal control signals without considering the system constraints causes the performance of these methods to decrease, especially in cases where the control commands reach the limit. The conditions under which the system is tested can be challenging for the aircraft and limitations and landings can be avoided in these situations, but the MPC solution offers a wider operating range.

Landing reference creation criteria are based on the aircraft not making sudden movements as much as possible, continuity was taken into account while reducing speed and altitude, and it was aimed by the designer that the derivative of the reference should not be zero.

Gain scheduling structure can be established with the gains obtained as a result of the linearization process to be performed at more than one point. In this study, the entire landing stage is considered around a point.

In the simulation examinations, the operating speed of the controller system was found to be sufficient, and it was integrated into a real flight control computer and made suitable for flight tests.

References

John H. Blakelock. (1991). *Automatic control of aircraft and missiles.* Book, John Wiley & Sons., 1991

Federal Aviation Administration. (2016) *Airplane Flying Handbook*, Standard,U.S. Department of Transportation, 2016

Mayne, D. Q., Rawlings, J. B., Rao, C. V., Scokaert, P. O. M. (2000) *Constrained model predictive control: Stability and optimality.*, Automatica, Vol.36

Military Standarts-USAF. (2008). *Flight Control Systems - Design, Installation and Test of Piloted Aircraft, General Specification for (MIL-DTL-9490E)*, Standard,U.S.A.F, 2008

Rossiter, J Anthony (2017) *Model-based predictive control: A practical approach. In Model-Based Predictive Control: A Practical Approach*, Book, 2017

Stevens, B. L., Lewis, F. L., Johnson, E. N. (2015) *Aircraft Control and Simulation: Dynamics, Controls Design, and Autonomous Systems: Third Edition*, Book, 2015

Wang, Liuping (2009) *Model Predictive Control System Design and Implementation Using MATLAB®*, Book, 2009

Wolowicz, C. H., Bowman, J. S., & Gilbert, W. P. (1979). *SIMILITUDE REQUIREMENTS AND SCALING RELATIONSHIPS AS APPLIED TO MODEL TESTING* Technical Paper, NASA Technical Paper, Issue 1435